

Rapid Bravais-lattice determination algorithm for lattice parameters containing large observation errors

R. Oishi-Tomiyasu

High Energy Accelerator Research Organization, Tsukuba, Ibaraki, Japan. Correspondence e-mail: ryoko.tomiyasu@kek.jp

Received 29 February 2012

Accepted 29 May 2012

A new Bravais-lattice determination algorithm is introduced herein. For error-stable Bravais-lattice determination, Andrews & Bernstein [*Acta Cryst.* (1988), **A44**, 1009–1018] proposed the use of operations to search for nearly Buerger-reduced cells. Although these operations play an essential role in their method, they increase the computation time, in particular when lattice parameters obtained in (powder) auto-indexing are supposed to contain large errors. The new algorithm requires only several permutation matrices in addition to the operations that are necessary when the lattice parameters have exact values. As a result, the computational efficiency of error-stable Bravais-lattice determination is improved considerably. Furthermore, the new method is proved to be error stable under a very general assumption. The detailed algorithms and the set of matrices sufficient for error-stable determination are presented.

© 2012 International Union of Crystallography
Printed in Singapore – all rights reserved

1. Introduction

In Bravais-lattice determination, using the parameter of a primitive cell, its corresponding Bravais type and the parameter of the conventional cell are determined. This process is required, for example, after auto-indexing of (powder) diffraction patterns. In general, a set of lattice parameters $a, b, c, \alpha, \beta, \gamma$ or a metric tensor (3-by-3 positive definite symmetric matrix) is used as the parameter of a three-dimensional lattice.

When a metric tensor of a lattice is Niggli reduced and has an exact value, it is known that the metric tensor belongs to a union of several linear spaces given by 44 lattice characters (Hahn, 1983; Niggli, 1928). However, if the metric tensor contains an observation error, as shown by Andrews & Bernstein (1988), sometimes it is not near the union set.

Studies on Bravais-lattice determination under experimental uncertainties have been conducted by Clegg (1981), Le Page (1982), Zimmermann & Burzlaff (1985) and Andrews & Bernstein (1988). Determination in the case of very small errors, such as computational rounding errors, has been discussed by Buerger (1957), Gruber (1973), Křivý & Gruber (1976), Zuo *et al.* (1995) and Grosse-Kunstleve *et al.* (2004).

Zimmermann & Burzlaff adopted the Delaunay reduction (Delaunay, 1933) because the number of lattice characters for the Delaunay reduction is 30, which is less than the 44 required for the Buerger reduction. Andrews & Bernstein (1988) assumed the use of the Buerger reduction and proposed the use of operations that provide nearly Buerger-reduced cells, in addition to the matrices associated with the 44 lattice characters. The former operations are computed by

multiplying the 25 Gruber operations recursively (Gruber, 1973). However, they did not clarify how many operations are required in the worst case.

In Appendix B in the supplementary material,¹ it is explained that 168 operations are required to give all the nearly Buerger-reduced cells in the worst case, which can occur even if the errors in the parameters are as small as rounding errors. As a result, more than a thousand operations are generated by multiplying these operations and the matrices. This is very time consuming for repeated execution after auto-indexing, in particular when many powder indexing solutions are found. Moreover, lattice parameters obtained by powder indexing usually contain large observation errors because of zero-point shift. This further affects the computation time.

The most effective way to reduce the time is to decrease the number of matrices used in error-stable determination. For this purpose, our algorithm applies the Minkowski reduction to cells with no centring (primitive), and the Delaunay reduction to face-centred, body-centred, rhombohedral and base-centred cells.

For primitive monoclinic, body-centred and face-centred orthorhombic cells, it is confirmed by Theorems 1 and 2 that only three permutation matrices are sufficient for error-stable determination as long as the errors in the metric tensors are not large enough for the following assumption to become false:

¹ Appendices A, B, C and D are available as supplementary material from the IUCr electronic archives (Reference: SC5050). Services for accessing these data are described at the back of the journal.

(A) If p satisfies $p \geq c_1|l_1|^2 + \dots + c_m|l_m|^2$ theoretically for some $c_i \geq \frac{1}{2}$ and lattice vectors $l_i \neq 0$ of a crystal lattice L (or its reciprocal lattice L^*), the observed value p^{obs} is also positive.

In simple terms, (A) assumes that $|l|^2$ and $\frac{1}{2}|l|^2$ are never observed as a negative value for any $0 \neq l \in L$ or L^* . Although (A) is considered to be true in normal experimental data, overestimation of errors may sometimes make (A) false in practical cases. This will be discussed in §5.4.

For rhombohedral and base-centred monoclinic cells, similar assertions are proved in Theorems 3 and 4. Furthermore, in Propositions 1 and 2, it is confirmed that only 16 and 21 matrices are required for these cells, respectively, if the nearest projection is prioritized, as in the case of Andrews & Bernstein (1988).

The determination of higher symmetries, including cubic, hexagonal, tetragonal and base-centred orthogonal cells, is almost straightforward after the type of centring is determined. The procedures for these symmetries are summarized in §5.3.

In §5.4, the advantages of the new algorithm are explained from a theoretical point of view. In particular, in the best case, the new method is more than 120 times faster than the existing method.

The new algorithm is implemented in the new powder auto-indexing software *Conograph* (Oishi-Tomiyasu & Kamiyama, 2011). §6 presents the results of Bravais-lattice determination using *Conograph*. Distribution of the Bravais-lattice determination module as a stand-alone program has not been planned thus far.

The Minkowski and Delaunay reductions are defined in §3. The definitions of Niggli and Buerger reductions are included in Appendix A. In §5.1, the linear subspaces to which metric tensors of a fixed centring type belong are presented, with explanations in §5.2. All the proofs of the theorems and propositions are provided in Appendices C and D, respectively.

Finally, we find that three operations among the 25 Gruber operations are redundant for determining the Niggli-reduced cells from the Buerger-reduced cells. This is mentioned in the last paragraph of Appendix B.

2. An inner product defined on the space of symmetric matrices

On the space $Sym^N(\mathbb{R})$ consisting of N -by- N symmetric matrices, an inner product is defined by

$$\langle S, T \rangle := \text{Trace}(ST) = \sum_{i=1}^N \sum_{j=1}^N s_{ij}t_{ij}. \quad (1)$$

For any $S \in Sym^N(\mathbb{R})$, $T \in Sym^M(\mathbb{R})$ and M -by- N real-valued matrix g , the following equations are obtained from $\text{Trace}(AB) = \text{Trace}(BA)$:

$$\text{if } N = M, \text{ then } \langle S, T \rangle = \langle T, S \rangle, \quad (2)$$

$$\langle gSg^T, T \rangle = \langle S, g^T Tg \rangle. \quad (3)$$

These inner products and equations are used in definitions and proofs.

3. Several facts in reduction theory

A three-dimensional lattice L with lattice parameters a, b, c, α, β and γ is associated with a 3-by-3 symmetric matrix having the following entries:

$$\begin{aligned} s_{11} &= a^2, & s_{22} &= b^2, & s_{33} &= c^2, \\ s_{12} &= ab \cos \gamma, & s_{13} &= ac \cos \beta, & s_{23} &= bc \cos \alpha. \end{aligned} \quad (4)$$

S is called a *metric tensor* of L and is also identified with a *quadratic form* of L .

As in the paper by Grosse-Kunstleve *et al.* (2004), the elements of the general linear group $GL(3, \mathbb{Z})$ are called change-of-basis matrices because they correspond to basis transforms of a lattice. The metric tensor S of L is not uniquely determined, because gSg^T is also a metric tensor of L for any change-of-basis matrix g . The reduction theory is necessary to resolve this ambiguity in the choice of S .

The Niggli and Buerger reductions, which are commonly used in crystallography, originated from the paper by Eisenstein (1851). Later, Minkowski established reduction theory for lattices of general dimension (Minkowski, 1905). Therefore, the definitions of these three reductions are very similar. The Delaunay reduction [also known as the Selling reduction (Selling, 1874)] is comparatively different from these reductions.

Below the definitions of the Minkowski and Delaunay reductions are provided in narrow and broad senses. In order to discuss Bravais-lattice determination methods, the Minkowski and Delaunay reductions in a broad sense are sometimes more convenient than those in a narrow sense because their corresponding domain is invariant by permutation matrices.

For any symmetry matrix S and change-of-basis matrix g , gSg^T is denoted by $S[g]$. The N -by- N identity matrix is denoted by I_N .

Minkowski-reduced domain. A metric tensor S of a lattice is *Minkowski reduced* if and only if it belongs to D_{\min} :

$$\begin{aligned} D_{\min} := \{ & (s_{ij})_{1 \leq i, j \leq 3} \in Sym^3(\mathbb{R}) : s_{11} \leq s_{22} \leq s_{33}, \\ & 2|s_{12}|, 2|s_{13}| \leq s_{11}, \quad 2|s_{23}| \leq s_{22}, \\ & 2|s_{13} + s_{23}| \leq s_{11} + s_{22} + 2s_{12}, \\ & 2|s_{13} - s_{23}| \leq s_{11} + s_{22} - 2s_{12} \}. \end{aligned} \quad (5)$$

Delaunay-reduced domain. For any 3-by-3 symmetric matrix $S := (s_{ij})_{1 \leq i, j \leq 3}$, let $\tilde{S} := (\tilde{s}_{ij})_{1 \leq i, j \leq 4}$ be the 4-by-4 symmetric matrix whose entries are given by

$$\begin{pmatrix} s_{11} & s_{12} & s_{13} & -\sum_{j=1}^3 s_{1j} \\ s_{21} & s_{22} & s_{23} & -\sum_{j=1}^3 s_{2j} \\ s_{31} & s_{32} & s_{33} & -\sum_{j=1}^3 s_{3j} \\ -\sum_{i=1}^3 s_{i1} & -\sum_{i=1}^3 s_{i2} & -\sum_{i=1}^3 s_{i3} & \sum_{i=1}^3 \sum_{j=1}^3 s_{ij} \end{pmatrix}. \quad (6)$$

This 4-by-4 symmetric matrix is frequently used to represent the Delaunay reduction cells, instead of S . The following relation formulas hold between S and \tilde{S} :

$$\tilde{S} = h_{\text{del}} S h_{\text{del}}^T, \quad (7)$$

$$S = h_0 \tilde{S} h_0^T, \quad (8)$$

$$h_{\text{del}} := \begin{pmatrix} 1 & 0 & 0 \\ 0 & 1 & 0 \\ 0 & 0 & 1 \\ -1 & -1 & -1 \end{pmatrix}, \quad (9)$$

$$h_0 := \begin{pmatrix} 1 & 0 & 0 & 0 \\ 0 & 1 & 0 & 0 \\ 0 & 0 & 1 & 0 \end{pmatrix}. \quad (10)$$

If $\tilde{S} \in \text{Sym}^4(\mathbb{R})$ corresponds to $S \in \text{Sym}^3(\mathbb{R})$ as equation (7), \tilde{S} belongs to the following subspace of $\text{Sym}^4(\mathbb{R})$:

$$V_{\text{del}} := \left\{ (\tilde{s}_{ij})_{1 \leq i, j \leq 4} \in \text{Sym}^4(\mathbb{R}) : \sum_{i=1}^4 \sum_{j=1}^4 \tilde{s}_{ij} = 0 \right\}. \quad (11)$$

S (or corresponding \tilde{S}) is said to be *Delaunay reduced* if and only if \tilde{S} belongs to D_{del} :

$$D_{\text{del}} := \left\{ (\tilde{s}_{ij})_{1 \leq i, j \leq 4} \in V_{\text{del}} : \tilde{s}_{11} \leq \tilde{s}_{22} \leq \tilde{s}_{33} \leq \tilde{s}_{44}, \right. \\ \left. \tilde{s}_{ij} \leq 0 \ (1 \leq i < j \leq 4) \right\}. \quad (12)$$

Minkowski-reduced domain in a broad sense. A metric tensor is *Minkowski reduced in a broad sense* if and only if it is an element of the following set:

$$\tilde{D}_{\text{min}} := \left\{ S \in \text{Sym}_{>0}^3(\mathbb{R}) : \langle S, I_3 \rangle = \min_{g \in GL(3, \mathbb{Z})} \langle S[g], I_3 \rangle \right\} \\ = \{ (s_{ij})_{1 \leq i, j \leq 3} \in \text{Sym}^3(\mathbb{R}) : 2|s_{ij}| \leq \min\{s_{ii}, s_{jj}\} \\ \text{and } 2|s_{ik} \pm s_{jk}| \leq s_{ii} + s_{jj} \pm 2s_{ij} \text{ for any} \\ 1 \leq i, j, k \leq 3 \text{ that differ from each other} \}. \quad (13)$$

It is well known in reduction theory that \tilde{D}_{min} contains D_{min} , and any $S \in \tilde{D}_{\text{min}}$ is transformed into an element of D_{min} by simply sorting its diagonal entries in ascending order using a permutation matrix.

Delaunay-reduced domain in a broad sense. A metric tensor is *Delaunay reduced in a broad sense* if and only if it is an element of the following set:

$$\tilde{D}_{\text{del}} := \left\{ \tilde{S} \in V_{\text{del}} : \langle \tilde{S}, I_4 \rangle = \min_{g \in GL(3, \mathbb{Z})} \langle \tilde{S}[g], I_4 \rangle \right\} \\ = \{ (\tilde{s}_{ij})_{1 \leq i, j \leq 4} \in V_{\text{del}} : \tilde{s}_{ij} \leq 0 \ (1 \leq i < j \leq 4) \}, \quad (14)$$

$$\tilde{S}[g] := (h_{\text{del}} g h_0) \tilde{S} (h_{\text{del}} g h_0)^T. \quad (15)$$

Clearly, D_{del} is contained in \tilde{D}_{del} .

From equations (3) and (7), the following equation is obtained:

$$\tilde{D}_{\text{del}} = \left\{ S \in \text{Sym}^3(\mathbb{R}) : \langle S, A_3 \rangle = \min_{g \in GL(3, \mathbb{Z})} \langle S[g], A_3 \rangle \right\}, \quad (16)$$

$$A_3 := h_{\text{del}}^T I_4 h_{\text{del}} = \begin{pmatrix} 2 & 1 & 1 \\ 1 & 2 & 1 \\ 1 & 1 & 2 \end{pmatrix}. \quad (17)$$

Any $\tilde{S} \in \tilde{D}_{\text{del}}$ is transformed into an element of D_{del} by $\tilde{S} \mapsto \tilde{S}[h_0 g h_{\text{del}}]$, using the 4-by-4 permutation matrix g that sorts the diagonal entries of \tilde{S} in ascending order.

For any subset $D \subset \text{Sym}^3(\mathbb{R})$ and a matrix g , a new domain $D[g]$ is defined as $\{gSg^T : S \in D\}$. The stabilizer subgroups of \tilde{D}_{min} , \tilde{D}_{del} , i.e. the sets of all $g \in GL(3, \mathbb{Z})$ with $\tilde{D}_{\text{min}}[g] = \tilde{D}_{\text{min}}$ and $\tilde{D}_{\text{del}}[g] = \tilde{D}_{\text{del}}$, coincide with the following groups, respectively:

$$St(I_3) := \{g \in GL(3, \mathbb{Z}) : g^T I_3 g = I_3\}, \quad (18)$$

$$St(A_3) := \{g \in GL(3, \mathbb{Z}) : g^T A_3 g = A_3\} \\ = \{h_0 g h_{\text{del}} : g \text{ is a 4-by-4 permutation matrix}\}. \quad (19)$$

The elements of $St(I_3)$ and $St(A_3)$ are listed in Tables 1 and 2.

4. Application of Minkowski reduction to monoclinic (P) cells

A monoclinic (P) lattice corresponds to a metric tensor $(s_{ij})_{1 \leq i, j \leq 3}$ contained in $V_{\text{mono}, p}$, a union of linear subspaces of $\text{Sym}^3(\mathbb{R})$:

$$V_{\text{mono}, p} := V_{\text{mono}, p, a} \cup V_{\text{mono}, p, b} \cup V_{\text{mono}, p, c}, \quad (20)$$

$$V_{\text{mono}, p, a} := \{(s_{ij})_{1 \leq i, j \leq 3} \in \text{Sym}^3(\mathbb{R}) : s_{12} = s_{13} = 0\}, \quad (21)$$

$$V_{\text{mono}, p, b} := \{(s_{ij})_{1 \leq i, j \leq 3} \in \text{Sym}^3(\mathbb{R}) : s_{12} = s_{23} = 0\}, \quad (22)$$

$$V_{\text{mono}, p, c} := \{(s_{ij})_{1 \leq i, j \leq 3} \in \text{Sym}^3(\mathbb{R}) : s_{13} = s_{23} = 0\}. \quad (23)$$

Any Buerger-reduced metric tensor belongs to $V_{\text{mono}, p}$ if it has precisely monoclinic (P) symmetry. However, if the observed metric tensor S^{obs} and the true metric tensor S do not become Buerger reduced with regard to the same basis, S^{obs} may not be close to $V_{\text{mono}, p}$, even if S^{obs} is Buerger reduced. Therefore, operations to search for nearly Buerger-reduced cells are necessary for error-stable determination.

However, if nearly monoclinic (P) cells are searched for instead of nearly Buerger-reduced cells, according to Theorem 1, such operations are not required by applying the Minkowski reduction.

Theorem 1. Let S^{obs} be an observed metric tensor of a lattice with monoclinic (P) symmetry, and let S be the true metric tensor corresponding to the same lattice basis as S^{obs} . Under assumption (A), if S^{obs} is Minkowski reduced in a broad sense, S belongs to $V_{\text{mono}, p}$.

The proof is found in Appendix C.

As a result, it is proved by Theorem 1 that the following algorithm is error stable because all the candidates permissible

Table 1

Elements of the stabilizer subgroup $St(I_3)$ in $GL(3, \mathbb{Z})$.

$$\begin{pmatrix} \pm 1 & 0 & 0 \\ 0 & \pm 1 & 0 \\ 0 & 0 & \pm 1 \end{pmatrix} \quad \begin{pmatrix} \pm 1 & 0 & 0 \\ 0 & 0 & \pm 1 \\ 0 & \pm 1 & 0 \end{pmatrix} \quad \begin{pmatrix} 0 & \pm 1 & 0 \\ \pm 1 & 0 & 0 \\ 0 & 0 & \pm 1 \end{pmatrix}$$

$$\begin{pmatrix} 0 & 0 & \pm 1 \\ \pm 1 & 0 & 0 \\ 0 & \pm 1 & 0 \end{pmatrix} \quad \begin{pmatrix} 0 & \pm 1 & 0 \\ 0 & 0 & \pm 1 \\ \pm 1 & 0 & 0 \end{pmatrix} \quad \begin{pmatrix} 0 & 0 & \pm 1 \\ 0 & \pm 1 & 0 \\ \pm 1 & 0 & 0 \end{pmatrix}$$

Table 2

Elements of the stabilizer subgroup $St(A_3)$ in $GL(3, \mathbb{Z})$.

$$\pm I_3 \quad \pm \begin{pmatrix} 0 & 0 & 1 \\ 1 & 0 & 0 \\ 0 & 1 & 0 \end{pmatrix} \quad \pm \begin{pmatrix} 0 & 1 & 0 \\ 0 & 0 & 1 \\ 1 & 0 & 0 \end{pmatrix}$$

$$\pm \begin{pmatrix} 1 & 0 & 0 \\ 0 & 0 & 1 \\ 0 & 1 & 0 \end{pmatrix} \quad \pm \begin{pmatrix} 0 & 0 & 1 \\ 0 & 1 & 0 \\ 1 & 0 & 0 \end{pmatrix} \quad \pm \begin{pmatrix} 0 & 1 & 0 \\ 1 & 0 & 0 \\ 0 & 0 & 1 \end{pmatrix}$$

$$\pm \begin{pmatrix} 1 & 0 & 0 \\ 0 & 1 & 0 \\ -1 & -1 & -1 \end{pmatrix} \quad \pm \begin{pmatrix} 1 & 0 & 0 \\ 0 & 0 & 1 \\ -1 & -1 & -1 \end{pmatrix} \quad \pm \begin{pmatrix} 0 & 1 & 0 \\ 0 & 0 & 1 \\ -1 & -1 & -1 \end{pmatrix}$$

$$\pm \begin{pmatrix} 0 & 1 & 0 \\ 1 & 0 & 0 \\ -1 & -1 & -1 \end{pmatrix} \quad \pm \begin{pmatrix} 0 & 0 & 1 \\ 1 & 0 & 0 \\ -1 & -1 & -1 \end{pmatrix} \quad \pm \begin{pmatrix} 0 & 0 & 1 \\ 0 & 1 & 0 \\ -1 & -1 & -1 \end{pmatrix}$$

$$\pm \begin{pmatrix} 1 & 0 & 0 \\ -1 & -1 & -1 \\ 0 & 1 & 0 \end{pmatrix} \quad \pm \begin{pmatrix} 1 & 0 & 0 \\ -1 & -1 & -1 \\ 0 & 0 & 1 \end{pmatrix} \quad \pm \begin{pmatrix} 0 & 1 & 0 \\ -1 & -1 & -1 \\ 0 & 0 & 1 \end{pmatrix}$$

$$\pm \begin{pmatrix} 0 & 1 & 0 \\ -1 & -1 & -1 \\ 1 & 0 & 0 \end{pmatrix} \quad \pm \begin{pmatrix} 0 & 0 & 1 \\ -1 & -1 & -1 \\ 1 & 0 & 0 \end{pmatrix} \quad \pm \begin{pmatrix} 0 & 0 & 1 \\ -1 & -1 & -1 \\ 0 & 1 & 0 \end{pmatrix}$$

$$\pm \begin{pmatrix} -1 & -1 & -1 \\ 1 & 0 & 0 \\ 0 & 1 & 0 \end{pmatrix} \quad \pm \begin{pmatrix} -1 & -1 & -1 \\ 1 & 0 & 0 \\ 0 & 0 & 1 \end{pmatrix} \quad \pm \begin{pmatrix} -1 & -1 & -1 \\ 0 & 1 & 0 \\ 0 & 0 & 1 \end{pmatrix}$$

$$\pm \begin{pmatrix} -1 & -1 & -1 \\ 0 & 1 & 0 \\ 1 & 0 & 0 \end{pmatrix} \quad \pm \begin{pmatrix} -1 & -1 & -1 \\ 0 & 0 & 1 \\ 1 & 0 & 0 \end{pmatrix} \quad \pm \begin{pmatrix} -1 & -1 & -1 \\ 0 & 0 & 1 \\ 0 & 1 & 0 \end{pmatrix}$$

Table 3

Algorithm for monoclinic (P) cells.

(Input) S^{obs} : Buerger-reduced metric tensor, †
 $\varepsilon > 0$: threshold,
 $\text{dist}(S, T)$: arbitrary distance function with arguments
 $S, T \in \text{Sym}^3(\mathbb{R})$.

(Output) A : array of pairs of a change-of-basis matrix g and
 $S \in V_{\text{mono},p,b}$ satisfying $\text{dist}(S, S^{\text{obs}}[g]) < \varepsilon$.

1: Prepare the array C_P of size $I_{\text{max}} := 3$:

$$C_P := \left\{ I_3, \begin{pmatrix} 1 & 0 & 0 \\ 0 & 0 & 1 \\ 0 & 1 & 0 \end{pmatrix}, \begin{pmatrix} 0 & 1 & 0 \\ 1 & 0 & 0 \\ 0 & 0 & 1 \end{pmatrix} \right\}.$$

2: for $i = 1$ to I_{max} do
 3: Compute $S_{\text{new}} := C_P[i] S^{\text{obs}} C_P[i]^T$ and
 4: Set

$$S := \begin{pmatrix} s_{11} & 0 & s_{13} \\ 0 & s_{22} & 0 \\ s_{13} & 0 & s_{33} \end{pmatrix},$$

where s_{ij} is the (i, j) entry of S_{new} .
 5: if $\text{dist}(S_{\text{new}}, S) < \varepsilon$, insert $(C_P[i], S)$ in A .
 6: end for

† Here it may be assumed that S^{obs} is Minkowski reduced in a broad sense.

by assumption (A) are checked in it. The three matrices used in Table 3 correspond to the projection of S^{obs} on each subspace, $V_{\text{mono},p,a}$, $V_{\text{mono},p,b}$ and $V_{\text{mono},p,c}$, respectively.

5. Application of Delaunay reduction to cases other than no-centring (primitive) type

While the Minkowski reduction is more suitable than the Buerger and Delaunay reductions for the determination of monoclinic (P) cells, the Delaunay reduction is more suitable than the Minkowski and Buerger reductions for face-centred, body-centred, rhombohedral and base-centred cells. This is because metric tensors corresponding to the latter Bravais types are basically contained in the interior of the Delaunay-reduced domain [equation (14)], while they belong to the boundary of the Minkowski-reduced domain [equation (13)] and Buerger-reduced domain [equation (61), see Appendix A].

5.1. Subspaces corresponding to lattice characters for Delaunay reduction

Here we shall define the subspaces of $\text{Sym}^3(\mathbb{R})$ in which the face-centred, body-centred, rhombohedral and base-centred lattices are supposed to be contained. Every subspace corresponds to a lattice character for the Delaunay reduction, except for the case of body-centred cells. Because the reciprocal lattice of a body-centred lattice has face-centred symmetry, a lattice character for face-centred cells is also applied to body-centred cells; this reduces the number of matrices used in the algorithm in §5.2.2; furthermore, it makes the determination of body-centred cells more error stable because metric tensors corresponding to a face-centred lattice

are never close to the boundary of the Delaunay-reduced domain [equation (14)].

5.1.1. Subspaces for face-centred cells. A face-centred cell in real space has a metric tensor belonging to

$$V_F := \{(s_{ij})_{1 \leq i, j \leq 3} : s_{12} = s_{13} = s_{23} = 0\}. \quad (24)$$

Hence, its primitive cell corresponds to the following metric tensor:

$$h_F \begin{pmatrix} a & 0 & 0 \\ 0 & b & 0 \\ 0 & 0 & c \end{pmatrix} h_F^T, \quad h_F := \frac{1}{2} \begin{pmatrix} 1 & 1 & 0 \\ 1 & -1 & 0 \\ -1 & 0 & 1 \end{pmatrix}. \quad (25)$$

As indicated by the lattice character for the Delaunay reduction, any Delaunay-reduced metric tensor \tilde{S} of a face-centred cell is an element of \tilde{V}_F defined by

$$\tilde{V}_F := \bigcup_{1 \leq k_1 < k_2 \leq 3} \tilde{V}_{F, k_1, k_2}, \quad (26)$$

$$\tilde{V}_{F, k_1, k_2} := \{(\tilde{s}_{ij})_{1 \leq i, j \leq 4} \in V_{\text{del}} : \tilde{s}_{k_1 l_1} = \tilde{s}_{k_1 l_2} = \tilde{s}_{k_2 l_1} = \tilde{s}_{k_2 l_2} \text{ for } 1 \leq l_1 < l_2 \leq 4 \text{ that differ from } k_1, k_2\}. \quad (27)$$

5.1.2. Subspaces for body-centred cells. If a conventional cell has a body-centred symmetry, the Delaunay-reduced metric tensor $\tilde{S} := (\tilde{s}_{ij})_{1 \leq i, j \leq 4}$ of its primitive cell in reciprocal space belongs to \tilde{V}_F defined by equation (26).

5.1.3. Subspaces for rhombohedral cells. If a lattice has rhombohedral symmetry, regardless of whether it is in real or reciprocal space, its metric tensor S is an element of V_R defined by

$$V_R := \{(s_{ij})_{1 \leq i, j \leq 3} : s_{11} = s_{22} = s_{33}, s_{12} = s_{13} = s_{23}\}. \quad (28)$$

The elements of V_R are positive definite but not Buerger reduced when $-\frac{1}{2}a < d < -\frac{1}{3}a$ or $\frac{1}{2}a < d < a$. On the other hand, the following linear space \tilde{V}_R contains every Delaunay-reduced metric tensor of a rhombohedral lattice:

$$\tilde{V}_R := \bigcup_{\substack{1 \leq k_1 < k_2 \leq 4 \\ 1 \leq l_1 \leq 4, l_1 \neq k_1, k_2}} \tilde{V}_{R, k_1, k_2, l_1}^+ \cup \bigcup_{1 \leq l_1 < l_2 < l_3 \leq 4} \tilde{V}_{R, l_1, l_2, l_3}^-, \quad (29)$$

$$\tilde{V}_{R, k_1, k_2, l_1}^+ := \{(\tilde{s}_{ij})_{1 \leq i, j \leq 4} \in V_{\text{del}} : \tilde{s}_{k_1 l_2} = \tilde{s}_{k_2 l_1} = 0, \tilde{s}_{k_1 k_2} = \tilde{s}_{k_1 l_1} = \tilde{s}_{k_2 l_2} \text{ for } 1 \leq l_2 \leq 4 \text{ that differs from } k_1, k_2, l_1\}, \quad (30)$$

$$\tilde{V}_{R, l_1, l_2, l_3}^- := \{(\tilde{s}_{ij})_{1 \leq i, j \leq 4} \in V_{\text{del}} : \tilde{s}_{l_1 l_1} = \tilde{s}_{l_2 l_2} = \tilde{s}_{l_3 l_3}, \tilde{s}_{l_1 l_2} = \tilde{s}_{l_1 l_3} = \tilde{s}_{l_2 l_3}\}. \quad (31)$$

5.1.4. Subspaces for base-centred cells. A base-centred cell has a metric tensor belonging to V_B :

$$V_B := \left\{ \begin{pmatrix} a & 0 & d \\ 0 & b & 0 \\ d & 0 & c \end{pmatrix} : a, b, c, d \in \mathbb{R} \right\}. \quad (32)$$

The following linear space \tilde{V}_B contains every Delaunay-reduced metric tensor of a base-centred lattice:

$$\tilde{V}_B := \bigcup_{1 \leq k_1 < k_2 \leq 4} \tilde{V}_{B, k_1, k_2}^{(1)} \cup \bigcup_{1 \leq k_1 < k_2 \leq 3} \tilde{V}_{B, k_1, k_2}^{(2)} \cup \bigcup_{1 \leq k_1, k_2 \leq 4} \tilde{V}_{B, k_1, k_2}^{(3)}, \quad (33)$$

$$\tilde{V}_{B, k_1, k_2}^{(1)} := \{(\tilde{s}_{ij})_{1 \leq i, j \leq 4} \in V_{\text{del}} : \tilde{s}_{k_1 l} = \tilde{s}_{k_2 l} \text{ for any } 1 \leq l \leq 4, l \neq k_1, k_2\}, \quad (34)$$

$$\tilde{V}_{B, k_1, k_2}^{(2)} := \{(\tilde{s}_{ij})_{1 \leq i, j \leq 4} \in V_{\text{del}} : \tilde{s}_{k_1 l} = \tilde{s}_{k_2 4}, \tilde{s}_{k_1 4} = \tilde{s}_{k_2 l} \text{ for } 1 \leq l \leq 3 \text{ that differ from } k_1, k_2\}, \quad (35)$$

$$\tilde{V}_{B, k_1, k_2}^{(3)} := \{(\tilde{s}_{ij})_{1 \leq i, j \leq 4} \in V_{\text{del}} : \tilde{s}_{k_1 k_2} = 0, \tilde{s}_{k_1 l_1} = \tilde{s}_{k_2 l_2} \text{ for } 1 \leq l_1 < l_2 \leq 4 \text{ that differ from } k_1, k_2\}. \quad (36)$$

This is seen from the following equations:

$$h_{\text{del}} h_B \begin{pmatrix} a & 0 & d \\ 0 & b & 0 \\ d & 0 & c \end{pmatrix} (h_{\text{del}} h_B)^T = \begin{pmatrix} \frac{a+b}{4} & \frac{a-b}{4} & \frac{d}{2} & -\frac{a+d}{2} \\ \frac{a-b}{4} & \frac{a+b}{4} & \frac{d}{2} & -\frac{a+d}{2} \\ \frac{d}{2} & \frac{d}{2} & c & -c-d \\ -\frac{a+d}{2} & -\frac{a+d}{2} & -c-d & a+c+2d \end{pmatrix}, \quad (37)$$

$$h_{\text{del}} T_B^{(2)} h_B \begin{pmatrix} a & 0 & d \\ 0 & b & 0 \\ d & 0 & c \end{pmatrix} (h_{\text{del}} T_B^{(2)} h_B)^T = \begin{pmatrix} \frac{a+b}{4} & \frac{-a+b}{4} & \frac{-a+b+2d}{4} & \frac{a-b+2d}{4} \\ \frac{-a+b}{4} & \frac{a+b}{4} & \frac{a-b+2d}{4} & \frac{-a+b+2d}{4} \\ -\frac{a+b+2d}{4} & \frac{a-b+2d}{4} & \frac{a+b}{4} + c + d & \frac{-a+b}{4} - c - d \\ \frac{a-b+2d}{4} & \frac{-a+b+2d}{4} & \frac{-a+b}{4} - c - d & \frac{a+b}{4} + c + d \end{pmatrix}, \quad (38)$$

Table 4

Algorithm for face-centred cells.

Note that, in this algorithm, the diagonal entries of the output matrices in A are not sorted.

- (Input) S^{obs} : Delaunay-reduced metric tensor of a lattice in real space, $\varepsilon > 0$, $\text{dist}(S, T)$: same as Table 3,
 (Output) A : array of pairs of an integer matrix g with $h_F g \in GL(3, \mathbb{Z})$ and a diagonal matrix S with $\text{dist}(S, S^{\text{obs}}[g]) < \varepsilon$.
 1: Prepare the inverse of h_F given by equation (25):

$$h_F^{-1} := \begin{pmatrix} 1 & 1 & 0 \\ 1 & -1 & 0 \\ 1 & 1 & 2 \end{pmatrix},$$

- 2: Prepare the array C_F of size $I_{\text{max}} := 3$:

$$C_F := \left\{ h_F^{-1}, h_F^{-1} \begin{pmatrix} 1 & 0 & 0 \\ 0 & 0 & 1 \\ 0 & 1 & 0 \end{pmatrix}, h_F^{-1} \begin{pmatrix} 0 & 1 & 0 \\ 0 & 0 & 1 \\ 1 & 0 & 0 \end{pmatrix} \right\}.$$

- 3: for $i = 1$ to I_{max} do
 4: Compute $S_{\text{new}} := C_F[i] S^{\text{obs}} C_F[i]^T$ and

$$S := \begin{pmatrix} s_{11} & 0 & 0 \\ 0 & s_{22} & 0 \\ 0 & 0 & s_{33} \end{pmatrix},$$
 where s_{ij} is the (i, j) entry of S_{new} .
 5: if $\text{dist}(S_{\text{new}}, S) < \varepsilon$, insert $(C_F[i], S)$ in A .
 6: end for

$$h_{\text{del}} T_B^{(3)} h_B \begin{pmatrix} a & 0 & d \\ 0 & b & 0 \\ d & 0 & c \end{pmatrix} (h_{\text{del}} T_B^{(3)} h_B)^T = \begin{pmatrix} \frac{a+b}{4} & \frac{d}{2} & -\frac{b}{2} & \frac{-a+b-2d}{4} \\ \frac{d}{2} & c & 0 & -c-\frac{d}{2} \\ -\frac{b}{2} & 0 & b & -\frac{b}{2} \\ \frac{-a+b-2d}{4} & -c-\frac{d}{2} & -\frac{b}{2} & \frac{a+b}{4} + c + d \end{pmatrix}, \quad (39)$$

where

$$h_B := \begin{pmatrix} \frac{1}{2} & \frac{1}{2} & 0 \\ \frac{1}{2} & -\frac{1}{2} & 0 \\ 0 & 0 & 1 \end{pmatrix}, \quad (40)$$

$$T_B^{(2)} := \begin{pmatrix} -1 & 0 & 0 \\ 0 & 1 & 0 \\ 1 & 0 & 1 \end{pmatrix}, \quad (41)$$

$$T_B^{(3)} := \begin{pmatrix} -1 & 0 & 0 \\ 0 & 0 & -1 \\ 1 & -1 & 0 \end{pmatrix}. \quad (42)$$

Table 5

Algorithm for body-centred cells.

- (Input) S^{obs} : metric tensor of a lattice in real space such that $(S^{\text{obs}})^{-1}$ is Delaunay reduced, $\varepsilon > 0$, $\text{dist}(S, T)$: same as Table 3,
 (Output) A : array of pairs of an integer matrix g with $h_I g \in GL(3, \mathbb{Z})$ and a diagonal matrix S with $\text{dist}(S, S^{\text{obs}}[g]) < \varepsilon$.
 1: Set the matrix h_I^{-1} :

$$h_I^{-1} := \begin{pmatrix} 1 & 1 & -1 \\ 1 & -1 & 0 \\ 0 & 0 & 1 \end{pmatrix},$$

- 2: Prepare the array C_I of size $I_{\text{max}} := 3$:

$$C_I := \left\{ h_I^{-1}, h_I^{-1} \begin{pmatrix} 1 & 0 & 0 \\ 0 & 0 & 1 \\ 0 & 1 & 0 \end{pmatrix}, h_I^{-1} \begin{pmatrix} 0 & 1 & 0 \\ 0 & 0 & 1 \\ 1 & 0 & 0 \end{pmatrix} \right\}.$$

- 3: for $i = 1$ to I_{max} do
 4: Compute $S_{\text{new}} := C_I[i] S^{\text{obs}} C_I[i]^T$ and

$$S := \begin{pmatrix} s_{11} & 0 & 0 \\ 0 & s_{22} & 0 \\ 0 & 0 & s_{33} \end{pmatrix},$$
 where s_{ij} is the (i, j) entry of S_{new} .
 5: if $\text{dist}(S_{\text{new}}, S) < \varepsilon$, insert $(C_I[i], S)$ in A .
 6: end for

5.2. Theorems and algorithms for lattice parameters containing observation errors

5.2.1. Face-centred cells. For face-centred lattices, the following theorem is obtained similarly to Theorem 1:

Theorem 2. Let \tilde{S}^{obs} be an observed metric tensor of a lattice with face-centred symmetry, and let \tilde{S} be the true metric tensor with regard to the same basis as \tilde{S}^{obs} . Under assumption (A), if \tilde{S}^{obs} is Delaunay reduced in a broad sense, \tilde{S} belongs to \tilde{V}_F defined by equation (26).

\tilde{V}_F is a union of three subspaces from equation (26). As a result of Theorem 2, the algorithm in Table 4 is proved to be error stable.

5.2.2. Body-centred cells. Except for the utilization of the metric tensor of a reciprocal lattice, this case is almost the same as the face-centred case. In particular, the algorithm in Table 5 is error stable.

5.2.3. Rhombohedral cells. For rhombohedral cells, the following theorem is obtained:

Theorem 3. Let \tilde{S}^{obs} be an observed metric tensor of a lattice with rhombohedral symmetry, and let \tilde{S} be the true metric tensor with regard to the same basis as \tilde{S}^{obs} . Under assumption (A), if \tilde{S}^{obs} is Delaunay reduced in a broad sense, \tilde{S} belongs to the following union of linear subspaces of V_{del} :

$$\tilde{V}_R \cup \bigcup_{g_0 \in St(A_3)} \tilde{V}_{R,1,2,3}^- [g_0 t_{001}] \cup \bigcup_{\substack{g_0 \in St(A_3) \\ h = t_{010} \cdot 001}} \tilde{V}_{R,1,2,3}^- [g_0 T_R^+ h], \quad (43)$$

where T_R^+ is defined by

Table 6

Change-of-basis matrices to search for nearly rhombohedral cells.

The matrices are chosen so that $\tilde{V}_{R,1,2,3}[g_1^{-1}] \neq \tilde{V}_{R,1,2,3}[g_2^{-1}]$ holds for any $g_1 \neq g_2$. Matrices in the first two rows of the table are contained in C_R .

$\begin{pmatrix} 1 & 0 & 0 \\ 0 & 1 & 0 \\ 0 & 0 & 1 \end{pmatrix}$	$\begin{pmatrix} 1 & 0 & 0 \\ 0 & 1 & 0 \\ -1 & -1 & -1 \end{pmatrix}$	$\begin{pmatrix} 1 & 0 & 0 \\ 0 & 0 & 1 \\ -1 & -1 & -1 \end{pmatrix}$	$\begin{pmatrix} 1 & 0 & 0 \\ 0 & 0 & -1 \\ 1 & 1 & 0 \end{pmatrix}$	$\begin{pmatrix} 1 & 0 & 0 \\ 0 & 0 & -1 \\ 0 & -1 & -1 \end{pmatrix}$	$\begin{pmatrix} 1 & 0 & 0 \\ 0 & -1 & 0 \\ 1 & 0 & 1 \end{pmatrix}$	$\begin{pmatrix} 1 & 0 & 0 \\ 0 & -1 & 0 \\ 0 & -1 & -1 \end{pmatrix}$	$\begin{pmatrix} 1 & 0 & 0 \\ 1 & 1 & 1 \\ 1 & 1 & 0 \end{pmatrix}$
$\begin{pmatrix} 1 & 0 & 0 \\ 1 & 1 & 1 \\ 1 & 0 & 1 \end{pmatrix}$	$\begin{pmatrix} 0 & 1 & 0 \\ 0 & 0 & 1 \\ -1 & -1 & -1 \end{pmatrix}$	$\begin{pmatrix} 0 & 1 & 0 \\ 0 & 0 & -1 \\ 1 & 1 & 0 \end{pmatrix}$	$\begin{pmatrix} 0 & 1 & 0 \\ 0 & 0 & -1 \\ -1 & 0 & -1 \end{pmatrix}$	$\begin{pmatrix} 0 & 1 & 0 \\ 1 & 1 & 1 \\ 1 & 1 & 0 \end{pmatrix}$	$\begin{pmatrix} 0 & 1 & 0 \\ 1 & 1 & 1 \\ 0 & 1 & 1 \end{pmatrix}$	$\begin{pmatrix} 0 & 0 & 1 \\ 1 & 1 & 1 \\ 1 & 0 & 1 \end{pmatrix}$	$\begin{pmatrix} 0 & 0 & 1 \\ 1 & 1 & 1 \\ 0 & 1 & 1 \end{pmatrix}$
$\begin{pmatrix} 1 & 0 & 0 \\ 0 & 0 & -1 \\ 0 & 1 & 1 \end{pmatrix}$	$\begin{pmatrix} 1 & 0 & 0 \\ 0 & 0 & -1 \\ -1 & -1 & 0 \end{pmatrix}$	$\begin{pmatrix} 1 & 0 & 0 \\ 0 & -1 & 0 \\ 0 & 1 & 1 \end{pmatrix}$	$\begin{pmatrix} 1 & 0 & 0 \\ 0 & -1 & 0 \\ -1 & 0 & -1 \end{pmatrix}$	$\begin{pmatrix} 1 & 0 & 0 \\ -1 & 0 & -1 \\ 1 & 1 & 1 \end{pmatrix}$	$\begin{pmatrix} 1 & 0 & 0 \\ -1 & -1 & 0 \\ 1 & 1 & 1 \end{pmatrix}$	$\begin{pmatrix} 0 & 1 & 0 \\ 0 & 0 & -1 \\ 1 & 0 & 1 \end{pmatrix}$	$\begin{pmatrix} 0 & 1 & 0 \\ 0 & 0 & -1 \\ -1 & -1 & 0 \end{pmatrix}$
$\begin{pmatrix} 0 & 1 & 0 \\ 0 & -1 & -1 \\ 1 & 1 & 1 \end{pmatrix}$	$\begin{pmatrix} 0 & 1 & 0 \\ -1 & -1 & 0 \\ 1 & 1 & 1 \end{pmatrix}$	$\begin{pmatrix} 0 & 0 & 1 \\ 0 & -1 & -1 \\ 1 & 1 & 1 \end{pmatrix}$	$\begin{pmatrix} 0 & 0 & 1 \\ -1 & 0 & -1 \\ 1 & 1 & 1 \end{pmatrix}$	$\begin{pmatrix} 1 & 0 & 0 \\ 0 & 1 & 0 \\ 0 & 0 & -1 \end{pmatrix}$	$\begin{pmatrix} 1 & 0 & 0 \\ 0 & 1 & 0 \\ 1 & 0 & 1 \end{pmatrix}$	$\begin{pmatrix} 1 & 0 & 0 \\ 0 & 1 & 0 \\ 0 & -1 & -1 \end{pmatrix}$	$\begin{pmatrix} 1 & 0 & 0 \\ 0 & 1 & 0 \\ 1 & 1 & 1 \end{pmatrix}$
$\begin{pmatrix} 1 & 0 & 0 \\ 0 & 0 & 1 \\ 0 & -1 & 0 \end{pmatrix}$	$\begin{pmatrix} 1 & 0 & 0 \\ 0 & 0 & 1 \\ 1 & 1 & 0 \end{pmatrix}$	$\begin{pmatrix} 1 & 0 & 0 \\ 0 & 0 & 1 \\ 0 & -1 & -1 \end{pmatrix}$	$\begin{pmatrix} 1 & 0 & 0 \\ 0 & 0 & 1 \\ 1 & 1 & 1 \end{pmatrix}$	$\begin{pmatrix} 1 & 0 & 0 \\ 0 & 0 & -1 \\ -1 & -1 & -1 \end{pmatrix}$	$\begin{pmatrix} 1 & 0 & 0 \\ 0 & -1 & 0 \\ -1 & -1 & -1 \end{pmatrix}$	$\begin{pmatrix} 1 & 0 & 0 \\ 1 & 1 & 0 \\ -1 & -1 & -1 \end{pmatrix}$	$\begin{pmatrix} 1 & 0 & 0 \\ 1 & 0 & 1 \\ -1 & -1 & -1 \end{pmatrix}$
$\begin{pmatrix} 1 & 0 & 0 \\ 0 & 1 & 0 \\ 0 & 1 & 1 \end{pmatrix}$	$\begin{pmatrix} 1 & 0 & 0 \\ 0 & 1 & 0 \\ -1 & 0 & -1 \end{pmatrix}$	$\begin{pmatrix} 1 & 0 & 0 \\ 0 & 0 & -1 \\ 0 & -1 & 0 \end{pmatrix}$	$\begin{pmatrix} 0 & 1 & 0 \\ 0 & 0 & 1 \\ 1 & 1 & 0 \end{pmatrix}$	$\begin{pmatrix} 0 & 1 & 0 \\ 0 & 0 & 1 \\ -1 & 0 & -1 \end{pmatrix}$	$\begin{pmatrix} 0 & 1 & 0 \\ 0 & 0 & 1 \\ 1 & 1 & 1 \end{pmatrix}$	$\begin{pmatrix} 0 & 1 & 0 \\ 0 & 0 & -1 \\ -1 & -1 & -1 \end{pmatrix}$	$\begin{pmatrix} 1 & 0 & 0 \\ 0 & -1 & 0 \\ 1 & 1 & 1 \end{pmatrix}$
$\begin{pmatrix} 0 & 1 & 0 \\ 1 & 1 & 0 \\ -1 & -1 & -1 \end{pmatrix}$	$\begin{pmatrix} 0 & 1 & 0 \\ 0 & 1 & 1 \\ -1 & -1 & -1 \end{pmatrix}$	$\begin{pmatrix} 1 & 0 & 0 \\ 0 & 0 & 1 \\ 0 & 1 & 1 \end{pmatrix}$	$\begin{pmatrix} 1 & 0 & 0 \\ 0 & 0 & 1 \\ -1 & -1 & 0 \end{pmatrix}$	$\begin{pmatrix} 0 & 1 & 0 \\ 0 & 0 & 1 \\ 1 & 0 & 1 \end{pmatrix}$	$\begin{pmatrix} 0 & 1 & 0 \\ 0 & 0 & 1 \\ -1 & -1 & 0 \end{pmatrix}$	$\begin{pmatrix} 0 & 1 & 0 \\ 0 & 0 & -1 \\ 1 & 1 & 1 \end{pmatrix}$	$\begin{pmatrix} 1 & 0 & 0 \\ 0 & 0 & -1 \\ 1 & 1 & 1 \end{pmatrix}$
$\begin{pmatrix} 0 & 0 & 1 \\ 1 & 0 & 1 \\ -1 & -1 & -1 \end{pmatrix}$	$\begin{pmatrix} 0 & 0 & 1 \\ 0 & 1 & 1 \\ -1 & -1 & -1 \end{pmatrix}$	$\begin{pmatrix} 0 & 0 & 1 \\ -1 & 0 & -1 \\ -1 & -1 & -1 \end{pmatrix}$	$\begin{pmatrix} 0 & 0 & 1 \\ 0 & -1 & -1 \\ -1 & -1 & -1 \end{pmatrix}$	$\begin{pmatrix} 0 & 1 & 0 \\ -1 & -1 & 0 \\ -1 & -1 & -1 \end{pmatrix}$	$\begin{pmatrix} 0 & 1 & 0 \\ 0 & -1 & -1 \\ -1 & -1 & -1 \end{pmatrix}$	$\begin{pmatrix} 1 & 0 & 0 \\ -1 & -1 & 0 \\ -1 & -1 & -1 \end{pmatrix}$	$\begin{pmatrix} 1 & 0 & 0 \\ -1 & 0 & -1 \\ -1 & -1 & -1 \end{pmatrix}$

$$T_R^+ := \begin{pmatrix} -1 & 0 & 0 \\ 0 & 1 & 0 \\ 1 & 0 & -1 \end{pmatrix}, \quad (44)$$

and t_{001} and t_{010} are diagonal matrices defined by

$$t_{i_1 i_2 i_3} := \begin{pmatrix} (-1)^{i_1} & 0 & 0 \\ 0 & (-1)^{i_2} & 0 \\ 0 & 0 & (-1)^{i_3} \end{pmatrix}. \quad (45)$$

The domain [equation (43)] is decomposed into the union $\bigcup_{g \in C_R} \tilde{V}_{R,1,2,3}[g^{-1}]$, where C_R is the set of the 64 matrices in Table 6. However, from the following proposition, it may be too prudent to use all the 64 matrices in order to search for nearly rhombohedral cells.

Proposition 1. Suppose that for an arbitrarily chosen $r > 0$, a distance on $Sym^3(\mathbb{R})$ is provided by

$$\text{dist}((s_{ij})_{1 \leq i, j \leq 3}, (t_{ij})_{1 \leq i, j \leq 3}) := \sum_{i=1}^3 (s_{ii} - t_{ii})^2 + r \sum_{1 \leq i < j \leq 3} (s_{ij} - t_{ij})^2. \quad (46)$$

In this case, the projection map $P_R : Sym^3(\mathbb{R}) \rightarrow V_R$ is defined by

$$\begin{pmatrix} s_{11} & s_{12} & s_{13} \\ s_{12} & s_{22} & s_{23} \\ s_{13} & s_{23} & s_{33} \end{pmatrix} \mapsto \frac{1}{3} \begin{pmatrix} a & d & d \\ d & a & d \\ d & d & a \end{pmatrix}, \quad (47)$$

$$a := \frac{s_{11} + s_{22} + s_{33}}{3}, \quad d := \frac{s_{12} + s_{13} + s_{23}}{3}.$$

The distance of the displacement $\delta_R(S) := \text{dist}(S, P_R(S))$ caused by the projection satisfies the following inequalities for

Table 7
Algorithm for rhombohedral cells.

(Input)	S^{obs} : Delaunay-reduced metric tensor, $\varepsilon > 0$, $\text{dist}(S, T)$: same as Table 3,
(Output)	A : array of pairs of a change-of-basis matrix g and $S \in V_{\mathbb{R}}$ satisfying $\text{dist}(S, S^{\text{obs}}[g]) < \varepsilon$.
1:	Prepare the array $C_{\mathbb{R}}^i$ of size $I_{\text{max}} := 16$ presented in Table 6.
2:	for $i = 1$ to I_{max} do
3:	Compute $S_{\text{new}} := C_{\mathbb{R}}^i S^{\text{obs}} C_{\mathbb{R}}^{iT}$.
4:	Set $a := \frac{1}{3}(s_{11} + s_{22} + s_{33})$ and $d := \frac{1}{3}(s_{12} + s_{13} + s_{23})$, using the (i, j) entry s_{ij} of S_{new} .
5:	Set $S := \begin{pmatrix} a & d & d \\ d & a & d \\ d & d & a \end{pmatrix}.$
6:	if $\text{dist}(S_{\text{new}}, S) < \varepsilon$, insert $(C_{\mathbb{R}}^i[i], S)$ in A .
7:	end for

any $g \in St(A_3)$ and 3-by-3 symmetric matrix S^{obs} with $h_{\text{del}} S^{\text{obs}} h_{\text{del}}^T \in \tilde{D}_{\text{del}}$:

$$\delta_{\mathbb{R}}(S^{\text{obs}}[g^{-1}]) \leq \delta_{\mathbb{R}}(S^{\text{obs}}[(gt_{001})^{-1}]), \quad (48)$$

$$\begin{aligned} \delta_{\mathbb{R}}(S^{\text{obs}}[(gT_{\mathbb{R}}^+)^{-1}]) &\leq \delta_{\mathbb{R}}(S^{\text{obs}}[(gT_{\mathbb{R}}^+ t_{001})^{-1}]) \\ &\leq \delta_{\mathbb{R}}(S^{\text{obs}}[(gT_{\mathbb{R}}^+ t_{010})^{-1}]). \end{aligned} \quad (49)$$

From Proposition 1, $P_{\mathbb{R}}(S^{\text{obs}}[g^{-1}])$ and $P_{\mathbb{R}}(S^{\text{obs}}[(gT_{\mathbb{R}}^+)^{-1}])$ are prioritized over $P_{\mathbb{R}}(S^{\text{obs}}[(gt_{001})^{-1}])$, $P_{\mathbb{R}}(S^{\text{obs}}[(gT_{\mathbb{R}}^+ t_{010})^{-1}])$ and $P_{\mathbb{R}}(S^{\text{obs}}[(gT_{\mathbb{R}}^+ t_{001})^{-1}])$ if the most feasible solution is determined by the distance between the observed metric tensor and its projection. This criterion was also used by Andrews & Bernstein (1988).

Therefore, the algorithm in Table 7 uses only the matrices belonging to the right cosets $St(A_3)$ and $St(A_3)T_{\mathbb{R}}^+$. They are given as the first 16 matrices in Table 6. We recommend the use of all 64 matrices only when a very prudent search is necessary.

5.2.4. Base-centred cells. For base-centred cells, the following theorem is obtained:

Theorem 4. Let \tilde{S}^{obs} be an observed metric tensor of a lattice with base-centred symmetry, and let \tilde{S} be the true metric tensor with regard to the same basis as \tilde{S}^{obs} . Under assumption (A), if \tilde{S}^{obs} is Delaunay reduced in a broad sense, \tilde{S} belongs to the following union of linear subspaces of V_{del} :

$$\tilde{V}_{\mathbb{B}} \cup \bigcup_{g_0 \in St(A_3)} \tilde{V}_{\mathbb{B},1,2}^{(1)}[g_0 t_{010}] \cup \bigcup_{\substack{g_0 \in St(A_3), \\ i=2,3}} \tilde{V}_{\mathbb{B},1,2}^{(1)}[g_0 T_{\mathbb{B}}^{(i)} \sigma_{23}], \quad (50)$$

where $T_{\mathbb{B}}^{(2)}, T_{\mathbb{B}}^{(3)}$ are the matrices defined by equations (41) and (42), respectively, and

$$\sigma_{23} := \begin{pmatrix} 1 & 0 & 0 \\ 0 & 0 & 1 \\ 0 & 1 & 0 \end{pmatrix}. \quad (51)$$

The domain of equation (50) is decomposed into the union $\bigcup_{g \in C_{\mathbb{B}}} \tilde{V}_{\mathbb{B},1,2}^{(1)}[g^{-1}]$, where $C_{\mathbb{B}}$ constitutes the 69 matrices in

Table 8. As in the case of rhombohedral cells, we have the following proposition:

Proposition 2. For a distance on $Sym^3(\mathbb{R})$ provided by equation (46) for some $r > 0$, the projection map $P_{\mathbb{B}} : Sym^3(\mathbb{R}) \rightarrow \tilde{V}_{\mathbb{B},1,2}^{(1)}$ is defined by

$$\begin{pmatrix} s_{11} & s_{12} & s_{13} \\ s_{12} & s_{22} & s_{23} \\ s_{13} & s_{23} & s_{33} \end{pmatrix} \mapsto \begin{pmatrix} a & s_{12} & d \\ s_{12} & a & d \\ d & d & s_{33} \end{pmatrix}, \quad a := \frac{s_{11} + s_{22}}{2}, \quad d := \frac{s_{13} + s_{23}}{2}. \quad (52)$$

The distance of the displacement $\delta_{\mathbb{B}}(S) := \text{dist}(S, P_{\mathbb{B}}(S))$ satisfies the following inequalities for any $g \in St(A_3)$ and 3-by-3 symmetric matrix S^{obs} with $h_{\text{del}} S^{\text{obs}} h_{\text{del}}^T \in \tilde{D}_{\text{del}}$:

$$\delta_{\mathbb{B}}(S^{\text{obs}}[g^{-1}]) \leq \delta_{\mathbb{B}}(S^{\text{obs}}[(gt_{010})^{-1}]), \quad (53)$$

$$\delta_{\mathbb{B}}(S^{\text{obs}}[(gT_{\mathbb{B}}^{(2)})^{-1}]) \leq \delta_{\mathbb{B}}(S^{\text{obs}}[(gT_{\mathbb{B}}^{(3)} \sigma_{23})^{-1}]), \quad (54)$$

$$\delta_{\mathbb{B}}(S^{\text{obs}}[(gT_{\mathbb{B}}^{(3)})^{-1}]) \leq \delta_{\mathbb{B}}(S^{\text{obs}}[(gT_{\mathbb{B}}^{(2)} \sigma_{23})^{-1}]). \quad (55)$$

In the algorithm in Table 9, we propose the use of only the matrices belonging to the right cosets $St(A_3)$, $St(A_3)T_{\mathbb{B}}^{(2)}$ and $St(A_3)T_{\mathbb{B}}^{(3)}$, as a result of Proposition 2. They correspond to the first 21 matrices in Table 8. In this case, the domain to search for nearly base-centred cells equals $\tilde{V}_{\mathbb{B}}$ defined by equation (33). As in the rhombohedral case, we recommend the use of all 69 matrices only when a very prudent search is necessary.

5.3. Algorithms for higher symmetries

After the centring type is determined, cells with higher symmetries are obtained from solutions of lower symmetries with the same centring type by basically following the same method as that described in Table 3. According to the symmetry, it is necessary to replace the set of used matrices and the projection map $S_{\text{new}} \mapsto S$.

The sets of matrices used are listed in Table 10. Finally, the numbers of matrices used for each Bravais type are summarized in Table 11.

5.4. Computational efficiency of the new method

In Bravais-lattice determination, if the remaining conditions are exactly the same, the computation time is considered to be proportional to the number of matrices used in each algorithm. Hence, computational efficiency is simply measured by the number of matrices.

In our algorithm, 58 matrices are used in order to obtain solutions for all the Bravais types.

With regard to the method of Andrews & Bernstein, the number of lattice characters belonging to non-triclinic Bravais lattices is 42. In addition, as proved in Appendix B, when the metric tensor is near a face-centred lattice, it is necessary to check more than 168 matrices in order to obtain all nearly Buerger-reduced cells. Consequently, more than

Table 8

Matrices to search for nearly base-centred cells.

The matrices are chosen so that $\tilde{V}_{B,1,2}[g_1^{-1}] \neq \tilde{V}_{B,1,2}[g_2^{-1}]$ holds for any $g_1 \neq g_2$. Matrices in the first two rows and the first five in the third row are contained in C_B^c .

$\begin{pmatrix} 1 & 1 & 0 \\ 1 & -1 & 0 \\ 0 & 0 & 1 \end{pmatrix}$	$\begin{pmatrix} 1 & 0 & 1 \\ 1 & 0 & -1 \\ 0 & 1 & 0 \end{pmatrix}$	$\begin{pmatrix} 1 & 0 & -1 \\ 1 & 0 & 1 \\ 0 & 1 & 1 \end{pmatrix}$	$\begin{pmatrix} 1 & -1 & 0 \\ 1 & 1 & 0 \\ 0 & 1 & 1 \end{pmatrix}$	$\begin{pmatrix} 2 & 1 & 0 \\ 0 & -1 & 0 \\ 0 & 0 & 1 \end{pmatrix}$	$\begin{pmatrix} 2 & 1 & 0 \\ 0 & -1 & 0 \\ -1 & -1 & -1 \end{pmatrix}$	$\begin{pmatrix} 2 & 0 & 1 \\ 0 & 0 & -1 \\ 0 & 1 & 0 \end{pmatrix}$	$\begin{pmatrix} 2 & 0 & 1 \\ 0 & 0 & -1 \\ -1 & -1 & -1 \end{pmatrix}$
$\begin{pmatrix} 1 & -1 & -1 \\ 1 & 1 & 1 \\ 0 & 1 & 0 \end{pmatrix}$	$\begin{pmatrix} 1 & -1 & -1 \\ 1 & 1 & 1 \\ 0 & 0 & 1 \end{pmatrix}$	$\begin{pmatrix} 2 & 1 & 1 \\ 0 & -1 & -1 \\ -1 & 0 & -1 \end{pmatrix}$	$\begin{pmatrix} 0 & -1 & -1 \\ 2 & 1 & 1 \\ 0 & 1 & 0 \end{pmatrix}$	$\begin{pmatrix} 0 & 1 & 1 \\ 0 & 1 & -1 \\ 1 & 0 & 0 \end{pmatrix}$	$\begin{pmatrix} 1 & 2 & 0 \\ -1 & 0 & 0 \\ 0 & 0 & 1 \end{pmatrix}$	$\begin{pmatrix} 1 & 2 & 0 \\ -1 & 0 & 0 \\ -1 & -1 & -1 \end{pmatrix}$	$\begin{pmatrix} 0 & 2 & 1 \\ 0 & 0 & -1 \\ 1 & 0 & 0 \end{pmatrix}$
$\begin{pmatrix} -1 & 1 & -1 \\ 1 & 1 & 1 \\ 1 & 0 & 0 \end{pmatrix}$	$\begin{pmatrix} -1 & 0 & -1 \\ 1 & 2 & 1 \\ 1 & 0 & 0 \end{pmatrix}$	$\begin{pmatrix} 1 & 0 & 2 \\ -1 & 0 & 0 \\ 0 & 1 & 0 \end{pmatrix}$	$\begin{pmatrix} 0 & 1 & 2 \\ 0 & -1 & 0 \\ 1 & 0 & 0 \end{pmatrix}$	$\begin{pmatrix} -1 & -1 & 0 \\ 1 & 1 & 2 \\ 1 & 0 & 0 \end{pmatrix}$	$\begin{pmatrix} 1 & 1 & 0 \\ 1 & -1 & 0 \\ 1 & 0 & 1 \end{pmatrix}$	$\begin{pmatrix} 1 & 1 & 0 \\ 1 & -1 & 0 \\ 0 & -1 & -1 \end{pmatrix}$	$\begin{pmatrix} 1 & 0 & 1 \\ 1 & 0 & -1 \\ 1 & 1 & 0 \end{pmatrix}$
$\begin{pmatrix} 1 & 0 & 1 \\ 1 & 0 & -1 \\ 0 & -1 & -1 \end{pmatrix}$	$\begin{pmatrix} 1 & 0 & -1 \\ 1 & 0 & 1 \\ 0 & 1 & 0 \end{pmatrix}$	$\begin{pmatrix} 1 & 0 & -1 \\ 1 & 0 & 1 \\ -1 & -1 & -1 \end{pmatrix}$	$\begin{pmatrix} 1 & -1 & 0 \\ 1 & 1 & 0 \\ 0 & 0 & 1 \end{pmatrix}$	$\begin{pmatrix} 1 & -1 & 0 \\ 1 & 1 & 0 \\ -1 & -1 & -1 \end{pmatrix}$	$\begin{pmatrix} 1 & 1 & 1 \\ 1 & -1 & -1 \\ 0 & 0 & -1 \end{pmatrix}$	$\begin{pmatrix} 0 & 0 & -1 \\ 2 & 0 & 1 \\ 0 & -1 & 0 \end{pmatrix}$	$\begin{pmatrix} 1 & 1 & 1 \\ 1 & -1 & -1 \\ 0 & -1 & 0 \end{pmatrix}$
$\begin{pmatrix} 0 & 0 & -1 \\ 2 & 0 & 1 \\ 1 & 1 & 1 \end{pmatrix}$	$\begin{pmatrix} 0 & -1 & 0 \\ 2 & 1 & 0 \\ 0 & 0 & -1 \end{pmatrix}$	$\begin{pmatrix} 0 & -1 & 0 \\ 2 & 1 & 0 \\ 1 & 1 & 1 \end{pmatrix}$	$\begin{pmatrix} 2 & 1 & 1 \\ 0 & -1 & -1 \\ 0 & 1 & 0 \end{pmatrix}$	$\begin{pmatrix} 2 & 1 & 1 \\ 0 & -1 & -1 \\ 0 & 0 & 1 \end{pmatrix}$	$\begin{pmatrix} 0 & -1 & -1 \\ 2 & 1 & 1 \\ 1 & 1 & 0 \end{pmatrix}$	$\begin{pmatrix} 0 & -1 & -1 \\ 2 & 1 & 1 \\ 1 & 0 & 1 \end{pmatrix}$	$\begin{pmatrix} 0 & 1 & 1 \\ 0 & 1 & -1 \\ 1 & 1 & 0 \end{pmatrix}$
$\begin{pmatrix} 0 & 1 & 1 \\ 0 & 1 & -1 \\ -1 & 0 & -1 \end{pmatrix}$	$\begin{pmatrix} 0 & 1 & -1 \\ 0 & 1 & 1 \\ 1 & 0 & 0 \end{pmatrix}$	$\begin{pmatrix} 0 & 1 & -1 \\ 0 & 1 & 1 \\ -1 & -1 & -1 \end{pmatrix}$	$\begin{pmatrix} 1 & 1 & 1 \\ -1 & 1 & -1 \\ 0 & 0 & -1 \end{pmatrix}$	$\begin{pmatrix} 1 & 1 & 1 \\ -1 & 1 & -1 \\ -1 & 0 & 0 \end{pmatrix}$	$\begin{pmatrix} 0 & 0 & -1 \\ 0 & 2 & 1 \\ -1 & 0 & 0 \end{pmatrix}$	$\begin{pmatrix} 0 & 0 & -1 \\ 0 & 2 & 1 \\ 1 & 1 & 1 \end{pmatrix}$	$\begin{pmatrix} -1 & 0 & 0 \\ 1 & 2 & 0 \\ 0 & 0 & -1 \end{pmatrix}$
$\begin{pmatrix} -1 & 0 & 0 \\ 1 & 2 & 0 \\ 1 & 1 & 1 \end{pmatrix}$	$\begin{pmatrix} 1 & 2 & 1 \\ -1 & 0 & -1 \\ 1 & 0 & 0 \end{pmatrix}$	$\begin{pmatrix} 1 & 2 & 1 \\ -1 & 0 & -1 \\ 0 & 0 & 1 \end{pmatrix}$	$\begin{pmatrix} -1 & 0 & -1 \\ 1 & 2 & 1 \\ 1 & 1 & 0 \end{pmatrix}$	$\begin{pmatrix} -1 & 0 & -1 \\ 1 & 2 & 1 \\ 0 & 1 & 1 \end{pmatrix}$	$\begin{pmatrix} 1 & 1 & 1 \\ -1 & -1 & 1 \\ 0 & -1 & 0 \end{pmatrix}$	$\begin{pmatrix} 1 & 1 & 1 \\ -1 & -1 & 1 \\ -1 & 0 & 0 \end{pmatrix}$	$\begin{pmatrix} 0 & -1 & 0 \\ 0 & 1 & 2 \\ -1 & 0 & 0 \end{pmatrix}$
$\begin{pmatrix} 0 & -1 & 0 \\ 0 & 1 & 2 \\ 1 & 1 & 1 \end{pmatrix}$	$\begin{pmatrix} -1 & 0 & 0 \\ 1 & 0 & 2 \\ 0 & -1 & 0 \end{pmatrix}$	$\begin{pmatrix} -1 & 0 & 0 \\ 1 & 0 & 2 \\ 1 & 1 & 1 \end{pmatrix}$	$\begin{pmatrix} 1 & 1 & 2 \\ -1 & -1 & 0 \\ 1 & 0 & 0 \end{pmatrix}$	$\begin{pmatrix} 1 & 1 & 2 \\ -1 & -1 & 0 \\ 0 & 1 & 0 \end{pmatrix}$	$\begin{pmatrix} -1 & -1 & 0 \\ 1 & 1 & 2 \\ 1 & 0 & 1 \end{pmatrix}$	$\begin{pmatrix} -1 & -1 & 0 \\ 1 & 1 & 2 \\ 0 & 1 & 1 \end{pmatrix}$	$\begin{pmatrix} 1 & 0 & 0 \\ 1 & 2 & 2 \\ 0 & 1 & 0 \end{pmatrix}$
$\begin{pmatrix} 1 & 0 & 0 \\ 1 & 2 & 2 \\ 0 & 0 & 1 \end{pmatrix}$	$\begin{pmatrix} 0 & 1 & 0 \\ 2 & 1 & 2 \\ 1 & 0 & 0 \end{pmatrix}$	$\begin{pmatrix} 0 & 1 & 0 \\ 2 & 1 & 2 \\ 0 & 0 & 1 \end{pmatrix}$	$\begin{pmatrix} 0 & 0 & 1 \\ 2 & 2 & 1 \\ 1 & 0 & 0 \end{pmatrix}$	$\begin{pmatrix} 0 & 0 & 1 \\ 2 & 2 & 1 \\ 0 & 1 & 0 \end{pmatrix}$			

$168 \times 42 = 7056$ matrices are required in the worst case. On the other hand, in the best case, *i.e.* when only one matrix among the 25 Gruber matrices gives a nearly Buerger-reduced cell, $25 + 42 = 67$ matrices are used in total.

Therefore, it is concluded that the new algorithm enhances efficiency up to about $7056/58 \simeq 121.7$ times, compared to the existing method.

Another advantage of the new method is that its efficiency is not affected by the overestimation of errors by users because the number of matrices is not magnified by the overestimation.

In the method of Andrews & Bernstein (1988), the number of matrices generated by the recursive use of Gruber operations is uncertain.

In general, condition (A) is supposed to be true, at least for correctly estimated errors in normal experimental data. In addition, as explained in Appendix B, if the assumption (A₀)

derived from assumption (A) is false, infinitely many matrices are required for error-stable Bravais-lattice determination theoretically. [(A₀) An observed metric tensor S^{obs} is sufficiently far from any 3-by-3 symmetric matrix that is not positive definite.]

Although it is not discussed here, it seems to be very plausible that (A) and (A₀) become equivalent conditions, depending on the distance function. Hence, it is natural that (A) is required in Bravais-lattice determination.

6. Application to powder indexing solutions

6.1. Implementation in Conograph

Fig. 1 shows the position of the Bravais-lattice determination in the flowchart of the powder indexing software *Conograph*.

Table 9

Algorithm for base-centred cells.

Note that output matrices in A are not transformed into Niggli-reduced form yet, i.e. some of them do not satisfy $0 \leq -d \leq \min\{a/2, c\}$.

(Input) S^{obs} : Delaunay-reduced metric tensor of a lattice in real space, $\varepsilon > 0$, $\text{dist}(S, T)$: same as Table 3,
 (Output) A : array of pairs of an integer matrix g with $h_B g \in GL(3, \mathbb{Z})$ and $S \in V_B$ satisfying $\text{dist}(S, S^{\text{obs}}[g]) < \varepsilon$.
 1: Prepare the array C_B^r of size $I_{\text{max}} := 21$ presented in Table 6.
 2: for $i = 1$ to I_{max} do
 3: Compute $S_{\text{new}} := C_B^r[i] S^{\text{obs}} C_B^r[i]^T$,
 4: Set

$$S := \begin{pmatrix} s_{11} & 0 & s_{13} \\ 0 & s_{22} & 0 \\ s_{13} & 0 & s_{33} \end{pmatrix},$$

using the (i, j) entry s_{ij} of S_{new} .
 5: if $\text{dist}(S_{\text{new}}, S) < \varepsilon$, insert $(C_B^r[i], S)$ in A .
 6: end for

Table 10

Matrices to obtain cells with higher symmetries.

Input cells	Output cells	Set of matrices
Monoclinic	Orthorhombic	I_3
Monoclinic (P)†	Hexagonal	$\begin{pmatrix} 1 & 0 & 0 \\ 0 & 0 & 1 \\ 0 & 1 & 0 \end{pmatrix}$
Orthogonal	Tetragonal	$I_3, \begin{pmatrix} 1 & 0 & 0 \\ 0 & 0 & 1 \\ 0 & 1 & 0 \end{pmatrix}, \begin{pmatrix} 0 & 1 & 0 \\ 1 & 0 & 0 \\ 0 & 0 & 1 \end{pmatrix}$
Orthogonal	Cubic	I_3

† The principal axis is supposed to be the b axis.

Table 11

Number of matrices required for each symmetry.

Bravais type	Number
Monoclinic (P), orthogonal (F, I), tetragonal (P, I)	3
Monoclinic (B)	21
Rhombohedral	16
Orthogonal (P, C), hexagonal, cubic (P, I, F)	1

After candidates for the metric tensor of the crystal primitive cell are enumerated by powder auto-indexing, they are transformed into Delaunay-reduced metric tensors by the Delaunay algorithm (Delaunay, 1933). The Buerger-reduced cells are easily constructed from the Delaunay-reduced metric tensors (Balashov & Ursell, 1957). Next, several figures of merit representing the reliability of powder indexing solutions are computed for each cell as a triclinic solution, and a part of the solutions are removed owing to low figures of merit [for example, de Wolff (1968) figure of merit $M_{20} < 2.0$]. Subsequently, Bravais-lattice determination is carried out.

Instead of a distance function and a threshold used in Tables 3–5, 7 and 9, *Conograph* judges if two metric tensors S^{obs} and S

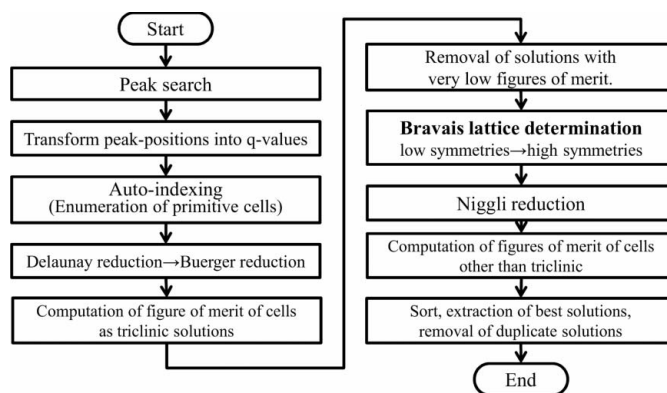


Figure 1
Flowchart of *Conograph*.

are close using error propagation based on approximated observation errors of peak positions as follows:

(1) *Estimation of errors in metric tensors.* In general, the peak positions are acquired using a peak-search program; hence, their errors are not obtained naturally. However, because statistics are essentially required for error-stable computation, the error (GErr) of a peak position is approximated in *Conograph* using the full width at half-maximum (FWHM) of the peak by

$$\text{GErr} := \frac{1}{(8 \log 2)^{1/2}} \text{FWHM}. \quad (56)$$

This formula equals the square root of the variance of the Gaussian distribution with the same FWHM. Subsequently, for powder patterns of angle dispersion, the q value of a peak position 2θ is computed as

$$q := \left(\frac{2}{\lambda} \sin \frac{2\theta + \Delta 2\theta}{2} \right)^2, \quad (57)$$

where λ is the wavelength of X-rays, 2θ is the diffraction angle of the peak position and $\Delta 2\theta$ is the zero-point shift. The propagation error of q is defined using the first derivative (linear approximation) by

$$\text{Err}[q] := \text{GErr} \times \frac{dq}{d2\theta} = \text{GErr} \times \frac{2q^{1/2}}{\lambda} \cos \frac{2\theta + \Delta 2\theta}{2}. \quad (58)$$

In the auto-indexing algorithm of *Conograph*, the entries of metric tensors S are obtained as a linear sum of q values. Therefore, the propagation error of S is defined similarly and computed from $\text{Err}[q]$.

(2) *Function to measure the difference between two metric tensors.* In the algorithms in the tables, the entries of S and S_{new} are defined as a linear sum of the entries of S^{obs} . The same holds for the entries ds_{ij} of $dS := S - S_{\text{new}}$. As a result, the propagation error $\text{Err}[ds_{ij}]$ of ds_{ij} is computed from that of S^{obs} . In *Conograph*, the formula used to judge whether S and S_{new} are close is given by

$$ds_{ij} \leq c \text{Err}[ds_{ij}] \text{ for all } 1 \leq i \leq j \leq 3, \quad (59)$$

where c is the tolerance level explained in the next paragraph.

(3) *Tolerance level c*. This parameter is used to set the scale of errors of the peak positions. The errors are approximated as $c \times \text{GErr}$. Considering the error caused by zero-point shift, the initial default value of c is set to 1 in *Conograph*. The test in §6.2 is executed with this value.

6.2. Results

Conograph has been tested with a variety of powder-diffraction patterns including all the Bravais types. In this section, the results for powder-diffraction patterns in Table 12 are presented.

In every case, success of the Bravais-lattice determination was confirmed using the correct solution of powder indexing. The time taken to carry out the determination was about 1.0×10^{-3} per metric tensor, as presented in Table 12.

In general, the determination is more time consuming when the crystal has higher symmetry. This is attributed to the increase in the number of Bravais lattices generated from a metric tensor. For example, when the algorithm in Table 3 is applied to an almost orthogonal (P) cell (*i.e.* s_{12} , s_{13} , s_{23} are rather small), three monoclinic (P) cells are generated as follows:

$$(s_{ij}) \mapsto \begin{pmatrix} s_{11} & 0 & s_{13} \\ 0 & s_{22} & 0 \\ s_{13} & 0 & s_{33} \end{pmatrix}, \begin{pmatrix} s_{11} & 0 & s_{12} \\ 0 & s_{33} & 0 \\ s_{12} & 0 & s_{22} \end{pmatrix}, \begin{pmatrix} s_{22} & 0 & s_{23} \\ 0 & s_{11} & 0 \\ s_{23} & 0 & s_{33} \end{pmatrix}. \quad (60)$$

As another example, when the algorithm in Table 9 is applied to a crystal lattice very close to a cubic (F) lattice, at least 11 monoclinic (B) cells are generated.

Unlike the method of Andrews & Bernstein, all the metric tensors satisfying equation (59) are enumerated, even in such a case. As a result, two cells having very close metric tensors are sometimes generated. This policy was adopted for powder indexing software. The process of extracting the best solutions using figures of merit and removing duplicates is carried out subsequently in *Conograph*.

7. Conclusion

A new Bravais-lattice determination algorithm was proposed, and this algorithm proved to be error stable under a general assumption that powder indexing solutions are considered to always satisfy. By applying Minkowski reduction and Delaunay reduction, the number of matrices used was reduced considerably. As a result, the new algorithm enhanced computational efficiency by more than 120 times, as compared

Table 12
Summary of test data.

Material	Source	Bravais type	Total time† (s)/number of metric tensors‡ = average time† (s)
Silicon	Spallation neutron	Cubic (F)	$1.44/1092 = 1.31 \times 10^{-3}$
Strontium iron oxide	Reactor neutron	Tetragonal (I)	$2.45/3134 = 0.78 \times 10^{-3}$
Alumina	Characteristic X-rays	Rhombohedral	$0.92/2249 = 0.41 \times 10^{-3}$
Acridol	Characteristic X-rays	Monoclinic (B)	$3.92/7050 = 0.56 \times 10^{-3}$

† The determination was carried out for every non-triclinic Bravais lattice, and the solutions were transformed into the Niggli-reduced cells during this time. The test was executed by parallel computing with eight hyper-threads using an Intel Core i7 CPU (3.20 GHz). ‡ This equals the number of solutions obtained by auto-indexing. As mentioned at the end of §6.2, solutions close to each other are generated in Bravais-lattice determination, and not only in auto-indexing. Because *Conograph* selects the best solutions and removes duplicates subsequently, the final solutions are much smaller than these numbers.

to the method of Andrews & Bernstein (1988). The new algorithm was implemented in the powder auto-indexing software *Conograph*.

References

- Andrews, L. C. & Bernstein, H. J. (1988). *Acta Cryst.* **A44**, 1009–1018.
 Balashov, V. & Ursell, H. D. (1957). *Acta Cryst.* **10**, 582–589.
 Buerger, M. J. (1957). *Z. Kristallogr.* **109**, 42–60.
 Clegg, W. (1981). *Acta Cryst.* **A37**, 913–915.
 Delaunay, B. (1933). *Z. Kristallogr.* **84**, 109–149.
 Eisenstein, G. (1851). *J. Reine Angew. Math.* **41**, 141–189.
 Grosse-Kunstleve, R. W., Sauter, N. K. & Adams, P. D. (2004). *Acta Cryst.* **A60**, 1–6.
 Gruber, B. (1973). *Acta Cryst.* **A29**, 433–440.
 Hahn, Th. (1983). *International Tables for Crystallography*, Vol. A. Dordrecht: Kluwer.
 Křivý, I. & Gruber, B. (1976). *Acta Cryst.* **A32**, 297–298.
 Le Page, Y. (1982). *J. Appl. Cryst.* **15**, 255–259.
 Minkowski, H. (1905). *J. Reine Angew. Math.* **129**, 220–274.
 Niggli, P. (1928). *Kristallographische und strukturtheoretische Grundbegriffe. Handbuch der Experimentalphysik*, Vol. 7. Leipzig: Akademische Verlagsgesellschaft.
 Oishi-Tomiyasu, R. & Kamiyama, T. (2011). *Acta Cryst.* **A67**, C205–C206.
 Selling, E. (1874). *J. Reine Angew. Math.* **77**, 143–229.
 Wolff, P. M. de (1968). *J. Appl. Cryst.* **1**, 108–113.
 Zimmermann, H. & Burzlaff, H. (1985). *Z. Kristallogr.* **170**, 241–246.
 Zuo, L., Muller, J., Philippe, M.-J. & Esling, C. (1995). *Acta Cryst.* **A51**, 943–945.